

TORC pathway intersects with a calcium sensor kinase network to regulate potassium sensing in Arabidopsis

Kun-Lun Li^a, Hui Xue^a, Ren-lie Tang^a, and Sheng Luan^{a,1}

Edited by Joseph Kieber, The University of North Carolina, Chapel Hill, NC; received September 14, 2023; accepted October 2, 2023

Potassium (K) is an essential macronutrient for plant growth, and its availability in the soil varies widely, requiring plants to respond and adapt to the changing K nutrient status. We show here that plant growth rate is closely correlated with K status in the medium, and this K-dependent growth is mediated by the highly conserved nutrient sensor, target of rapamycin (TOR). Further study connected the TOR complex (TORC) pathway with a low-K response signaling network consisting of calcineurin B-like proteins (CBL) and CBL-interacting kinases (CIPK). Under high K conditions, TORC is rapidly activated and shut down the CBL-CIPK low-K response pathway through regulatory-associated protein of TOR (RAPTOR)-CIPK interaction. In contrast, low-K status activates CBL-CIPK modules that in turn inhibit TORC by phosphorylating RAPTOR, leading to dissociation and thus inactivation of the TORC. The reciprocal regulation of the TORC and CBL-CIPK modules orchestrates plant response and adaptation to K nutrient status in the environment.

calcium signaling | protein kinases | nutrient sensing | TOR

Plant growth requires a number of mineral nutrients, including nitrogen-phosphoruspotassium (NPK) as the three macronutrients. While N and P are metabolized into various organic compounds essential for numerous biochemical processes, K⁺ functions in its ionic form in osmoregulation, enzyme activation, and maintenance of membrane potential among other processes (1, 2). Because NPK status in natural soils often becomes a limiting factor for plant growth, use of chemical fertilizers has been a critical practice to enhance crop productivity and quality in modern agriculture (3, 4). However, heavy use of fertilizers is deemed unsustainable because production of fertilizers is costly and pollutes environment (5-8). Understanding how plants sense and respond to nutrient status is essential for breeding effort to increase nutrient use efficiency and contribute to green agriculture.

While K⁺ concentration in soils is often in the submillimolar range, plant cells contain at least 100 mM K^{+} in the cytoplasm in order to support normal metabolism (1, 9–12). Plants have thus evolved many transporting proteins to enrich K⁺ and mechanisms to monitor and respond to the changing K status in the soil. In response to a low-K environment, plants utilize two Ca²⁺-CBL-CIPK pathways to activate K transport systems to maintain K homeostasis in plant cells. Specifically, CBL1 and CBL9 recruit CIPK1/9/23 to the plasma membrane where they function together to promote K uptake by phosphorylating and activating K channels and carriers such as AKT1 and HAK5 (13-17). In parallel, CBL2 and CBL3 function together with four CIPKs, CIPK3/9/23/26, at the vacuolar membrane where they initiate K remobilization from vacuolar stores by activating two pore K-channels (TPKs) (18). Among the two pathways, the tonoplast CBL2/3-CIPK pathway for K remobilization appears to serve as a primary mechanism for plants to cope with K-deficiency (18, 19). We previously showed that the CBL-CIPK network components in plants are fine-tuned in response to K status: They become more abundant and more active under low K and degraded when K levels are high (19). However, little is known about the upstream regulators of CBL-CIPK modules in plants under changing

The target of the rapamycin complex (TORC) is an evolutionarily conserved master regulator that connects various environmental and internal signals to promote growth (20-25). TORC in Arabidopsis contains the TOR kinase subunit and two accessory proteins, RAPTOR (regulatory-associated protein of TOR), which recruits substrates and presents them to TOR for phosphorylation, and LST8 (lethal with Sec thirteen 8), which stabilizes the TORC (26–29). In Arabidopsis, two RAPTOR isoforms, RAPTOR1A and RAPTOR1B, have been identified, and RAPTOR1B is believed to be the major RAPTOR isoform in the TORC (27, 30, 31). In yeast and mammals, TORC signaling pathways have been extensively studied and shown to connect energy and nutrient status

Significance

Low nutrient status in soils is often limiting to plant growth, making the use of fertilizers a necessity in crop production. However, heavy use of fertilizers is costly and pollutes environment. Understanding how plants respond and adapt to changing nutrient status is critical for breeding effort to increase nutrient use efficiency and cut fertilizers. This paper describes a mechanism that allows plants to adjust growth based on external potassium (K) status. High-K activates the target of rapamycin complex (TORC) pathway that in turn inactivates the low-Kresponsive calcineurin B-like proteins (CBL)-CBL-interacting kinases (CIPK) network, whereas K-deficiency turns on the CBL-CIPK network that inhibits the TORC pathway, underlying transitions between adaptation and growth promotion in plants depending on K availability.

Author affiliations: ^aDepartment of Plant and Microbial Biology, University of California, Berkeley, CA 94720

Author contributions: K.-L.L. and S.L. designed research; K.-L.L., H.X., and R.-J.T. performed research; H.X. and R.-J.T. contributed new reagents/analytic tools; K.-L.L. and S.L. analyzed data; and K.-L.L. and S.L. wrote the paper.

The authors declare no competing interest.

This article is a PNAS Direct Submission.

Copyright © 2023 the Author(s). Published by PNAS. This article is distributed under Creative Commons Attribution-NonCommercial-NoDerivatives License 4.0

¹To whom correspondence may be addressed. Email: sluan@berkeley.edu.

This article contains supporting information online at https://www.pnas.org/lookup/suppl/doi:10.1073/pnas. 2316011120/-/DCSupplemental.

Published November 15, 2023.

to cell growth (32, 33). Emerging studies in plants have revealed that TORC can be activated by a number of nutrient signals, including organic compounds (e.g., sugars, amino acids, nucleotides) and inorganic nutrients (e.g., nitrogen salts, phosphate, and sulfate) (22, 34–38). However, very little is known about the relationship between K nutrient status and TORC signaling although K^{+} is the most abundant cation and an essential nutrient in plant cells (1).

In this study, we identified a crosstalk between the TORC pathway and CBL—CIPK network in response to changing K levels in the medium. Transfer of plants from low- to high-K rapidly activates TOR that triggers CBL—CIPK dephosphorylation and degradation, to switch to growth mode. Upon exposure to K deficiency, plants initiate activation of the CBL—CIPK network that phosphorylates RAPTOR, resulting in a downturn of TOR activity and shifting to low-K response. This crosstalk between TORC and CBL—CIPK signal network thus enables plants to respond to changing K status in the soil and switch between growth and adaptation modes.

Results

K Activates the TORC to Promote Plant Growth. Plant growth requires sufficient K in the medium. To determine whether Kdependent growth requires TOR, we tested the effect of TOR suppression on plant growth in response to changing external K levels. Given embryonic lethality of tor null mutants (39), we performed this assay with an estradiol-induced TOR knockdown line (es-tor) of Arabidopsis (40). In the absence of the inducer estradiol, the growth of es-tor seedlings, like the wild type, was correlated with increasing K^+ levels (Fig. 1 A–C). In the presence of estradiol in the medium to induce TOR suppression, K-dependent growth of es-tor seedlings was almost completely abolished while the wild-type plants were not affected (Fig. 1 A–C). We then assessed plant growth in two raptor 1b knockout mutants, raptor 1-1 and raptor1-2, with decreased TOR activity (41) and found that K-responsive growth in both mutants were significantly reduced (Fig. 1 D-F). These results indicated that the TORC plays an essential role in K-dependent plant growth.

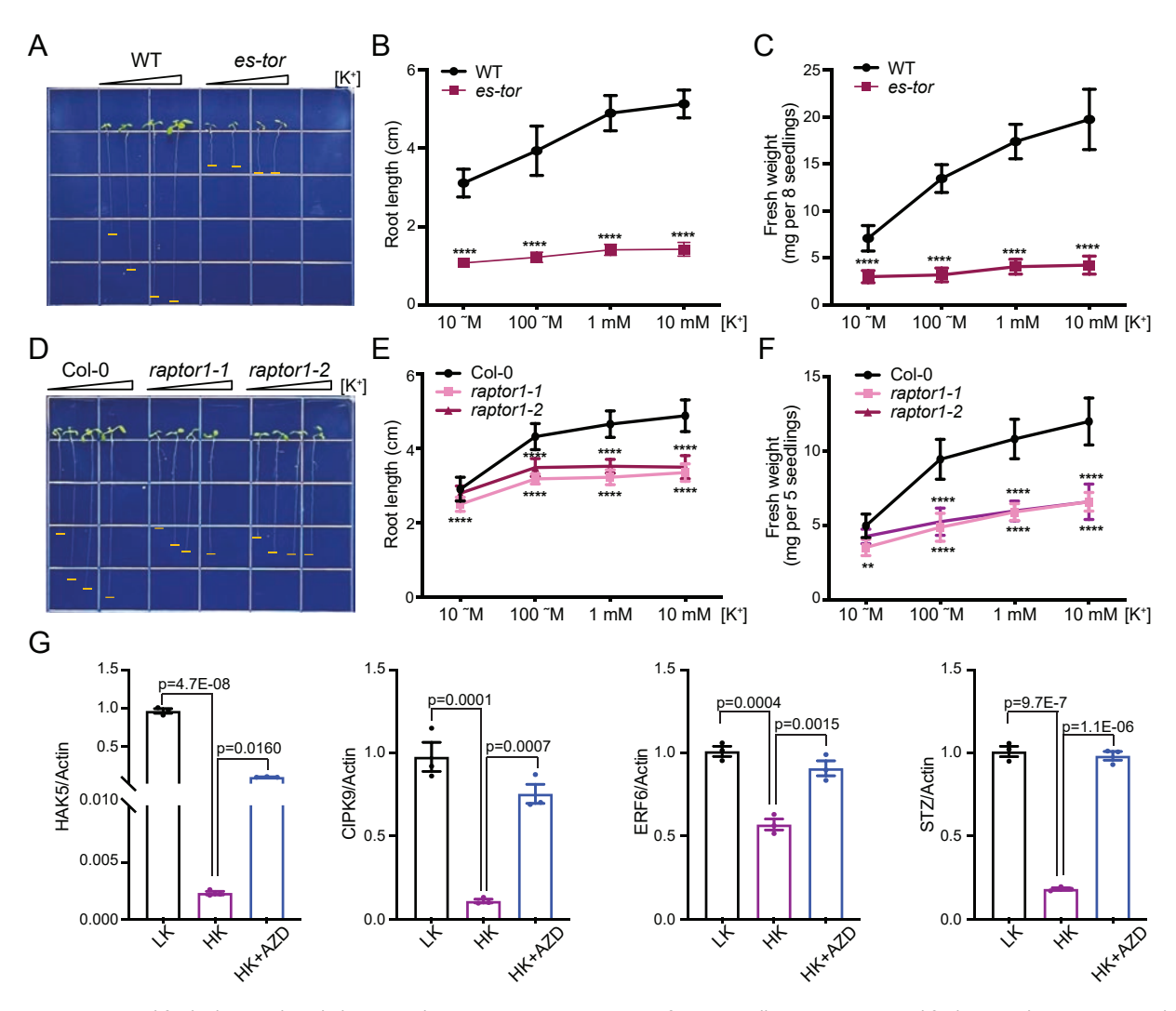


Fig. 1. TORC is required for high-K-mediated plant growth. (*A*) Representative images of *es-tor* seedlings grown on modified MS medium containing different concentrations of K⁺ (0.01, 0.1, 1, 10 mM) without or with estradiol for 7 d. (*B* and *C*) Root length and fresh weight measured at the end of the assay shown in (*A*). (*D*) Representative images of Col, *raptor1b* seedlings grown on modified MS medium containing different concentrations of K⁺ (0.01, 0.1, 1, 10 mM) for 7 d. (*E* and *F*) Root length and fresh weight measured at the end of the assay shown in (*D*). In (*B*, *C*, *E*, and *F*), data are mean ± SD of three biological replicates (*n* ≥ 26 seedlings). Asterisks indicate statistically significant differences compared with the wild type by two-way ANOVA followed by Sidak's multiple comparisons test. **P < 0.01, ****P < 0.0001. (*G*) Quantitative RT-PCR analysis of *HAK5*, *CIPK9*, *ERF6*, and *STZ* transcripts in response to low- to high-K or high-K plus AZD transition. The 5-d-old seedlings of Col-0 germinated on low-K medium were transferred to low-K, high-K, or high-K plus AZD (2 μM) for 1 d. The relative expression of *HAK5*, *CIPK9*, *ERF6*, or *STZ* was normalized against the expression of *ACTIN 2*. Data are shown as mean ± SEM, *n* = 3 (biologically independent experiments). Statistical analyses between groups were calculated by one-way ANOVA followed by Tukey's multiple comparison test.

TORC has been shown to promote growth by orchestrating global transcriptional reprogramming (22, 42). As K-mediated plant growth requires TORC (Fig. 1), we hypothesized that TORC may play a role in transcriptional regulation of K-responsive genes. Previous work showed that HAK5, CIPK9, ERF6, and STZ are upregulated in Arabidopsis response to K deficiency (18, 19, 43, 44). Consistently, these genes were dramatically downregulated in response to low- to high-K transition (Fig. 1G). If TORC was required for high K response in plants, the down-regulation of these low-K gene markers would not happen if TORC activity was blocked. Indeed, with the addition of AZD8055 to the medium to inhibit TORC, we observed blockade of high K-dependent repression of HAK5, CIPK9, ERF6, and STZ (Fig. 1G). These data support the conclusion that TORC is required for K response at the transcriptional level, which may contribute to K-dependent growth in Arabidopsis.

If K-dependent plant growth requires TORC activity, it is possible that K status may be monitored by a mechanism connected to the TORC pathway in plant cells. To investigate whether the TOR-kinase activity varies in response to changing external K levels, we measured TOR activity by examining the phosphorylation level of S6K1-T449 in seedlings upon high- to low-K transfer, or vice versa. The S6K1 (ribosomal S6 kinase 1) is a well-known TOR substrate that controls translation and growth, and S6K1 phosphorylation at Thr449 has been utilized as a reliable readout for TOR activity in Arabidopsis (22, 40). We found that the reactivation of TOR in plants upon low- to high-K transfer happened very rapidly upon K repletion (Fig. 2 A and B). Such activation was completely blocked by Torin2, a TOR-specific inhibitor (Fig. 2 A and B)(45). We further characterized the dose dependence and time course of K-mediated TOR activation and found that 30-min treatment with 1 mM

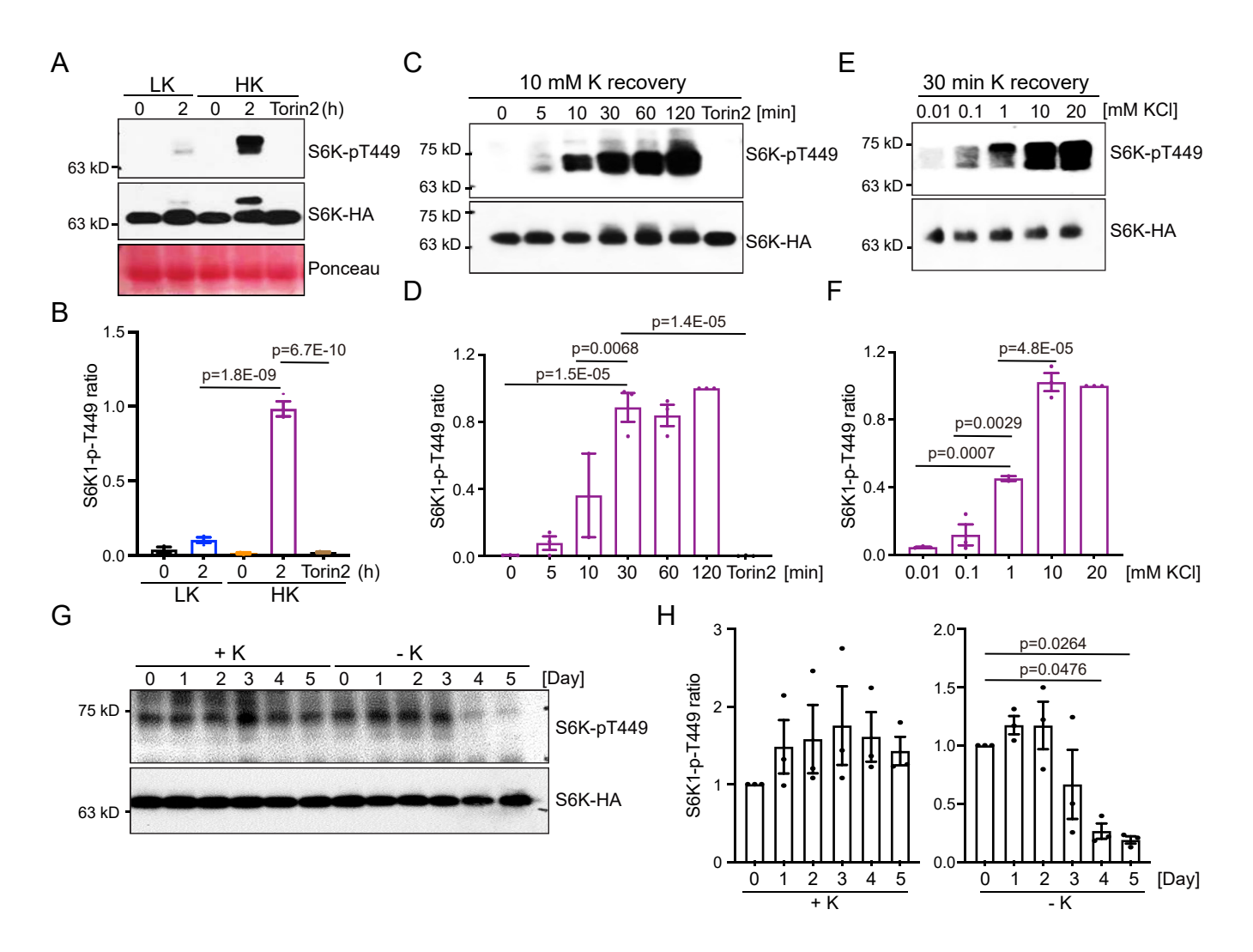


Fig. 2. K repletion activates whereas K deficiency inhibits TORC signaling. (A) TORC activity measured with anti-p-T449 of S6K1 in western blots. Transgenic *Arabidopsis* plants expressing 35S:S6K1-HA were grown on low-K medium for 8 d before being transferred to either low-K (10 μM) or high-K (20 mM) liquid medium for 2 h. Anti-HA (S6K1-HA) and Ponceau staining were used as loading controls. (B) Relative p-T449 intensity was calculated as the ratio of intensity of p-T449 over S6K1-HA. The value for the sample "HK 2 h" was set as 1. (C) Time course of K-mediated TOR activation. The 8-d-old seedlings of 35S:S6K1-HA germinated on low-K medium were transferred to high-K medium for indicated times. (D) Quantification of relative p-T449 intensity in (C). The value at 120 min was set as 1. (E) Dose dependence of K-mediated TOR activation. Seeds of transgenic line harboring 35S:S6K1-HA were germinated and grown on low-K medium for 8 d before being treated in liquid medium with different K concentrations for 30 min. (F) Quantification of relative p-T449 intensity in (E). The value of "20 mM" was set as 1. (G) TORC activity decreased in response to K deficiency. The 8-d-old seedlings of 35S:S6K1-HA germinated on high-K medium (2 mM) were transferred to low-K medium for the indicated time (days). TORC activity was based on p-T449 of S6K1 in western blots. Anti-HA (S6K1-HA) was used as a loading control. (H) Quantification of relative p-T449 intensity in (G). The data represent the ratio of intensity of p-T449 over S6K1-HA, and the value of "0 d" was set as 1. In (B, D, F, and H), data are means ± SEM, n = 3 (biologically independent experiments). Statistical analyses between groups were performed by one-way ANOVA followed by Tukey's multiple comparison test.

K was sufficient for inducing TOR activation, although a higher concentration of K (10 mM or 20 mM) further enhanced TOR activity (Fig. 2 *C–F*). Furthermore, we found that TOR-kinase activities remained high under sufficient K and showed a significant drop after 4 d of K deprivation treatment (Fig. 2 *G* and *H*), consistent with our previous finding that K starvation takes effect only after an extended period when stored K was depleted (19). Together, these data strongly suggest that TOR activation is an early response to high K nutrient status and may underlie K-dependent plant growth.

TORC Inhibits the Ca-dependent Low-K Response Network. While TORC is critical for high K-mediated plant growth, the CBL-CIPK pathways are required for low-K response for plant survival (13-18). In particular, the tonoplast CBL2/3-CIPK3/9/23/26 pathway functions as the primary mechanism for plants to respond and adapt to low-K stress (18, 19). Interestingly, the activities of TORC and CBL-CIPK are both responsive to changing K status although in an opposite direction: High K activates TORC (Fig. 2) but inactivates CBL-CIPK (19). We thus began to explore the possible relationship of the TORC pathway and CBL-CIPK network in plants under changing K status. Because high Kinduced activation of TORC happens earlier than the inactivation of the CBL-CIPK pathway (Fig. 2) (19), we hypothesized that TORC activation could be upstream of and required for CBL-CIPK inactivation. To test this possibility, we first examined the effect of TOR suppression in the es-tor plants on CBL-CIPK activity using CBL phosphorylation and protein abundance as readouts (19). Upon low- to high-K transfer without estradiol induction, es-tor seedlings, like the wild-type control, showed a typical high K-induced decrease in CBL2/3 phosphorylation and protein levels (Fig. 3A) (19). Upon application of estradiol to

knockdown TORC, CBL2/3 phosphorylation and protein levels in *es-tor* seedlings failed to decrease under high-K treatment for 3 d (Fig. 3A). Similarly, high-K-induced dephosphorylation and degradation of CBL2/3 was inhibited by the addition of TOR inhibitor AZD8055 (*SI Appendix*, Fig. S1). These results suggested that TOR is required for K-dependent CBL—CIPK inactivation.

We then tested whether inhibition of TOR activity is sufficient to mimic low-K activation of CBL-CIPK. Consistent with the earlier study (19), CBL2/3 phosphorylation and protein levels were induced by low-K treatment in wild-type seedlings (SI Appendix, Fig. S2). In contrast, seedlings grown under high K showed a minimal level of CBL2/3 proteins (Fig. 3B and SI Appendix, Fig. S2). Interestingly, when es-tor seedlings were grown under high K in the presence of estradiol to suppress TOR, CBL2/3 phosphorylation and accumulation were strongly elevated, recapitulating the degree of CBL-CIPK activation under low-K condition (Fig. 3B and SI Appendix, Fig. S2). Similarly, the addition of TOR inhibitor AZD8055 induced CBL2/3 phosphorylation even in the presence of high-K (SI Appendix, Fig. S3 A and B). Moreover, two independent lines of raptor 1b mutant grown under a high-K condition also showed a much higher CBL2/3 phosphorylation level compared to wild-type seedlings (Fig. 3C). In parallel with the change of phosphorylation, CBL2/3 protein level was also elevated in estradiol-treated es-tor and raptor1b seedlings even under high level of K supply (Fig. 3 B and C). Furthermore, we tested whether LK-activated CBL2/3 phosphorylation and protein accumulation are repressed in TOR overexpression plants, G548 and S7817 (46). As shown in SI Appendix, Fig. S4, G548 and S7817 plants exhibited a drastic decrease in CBL2/3 phosphorylation compared to wild-type seedlings under low-K conditions. Additionally, the low-K-induced increase in CBL2/3 protein abundance was notably reduced in

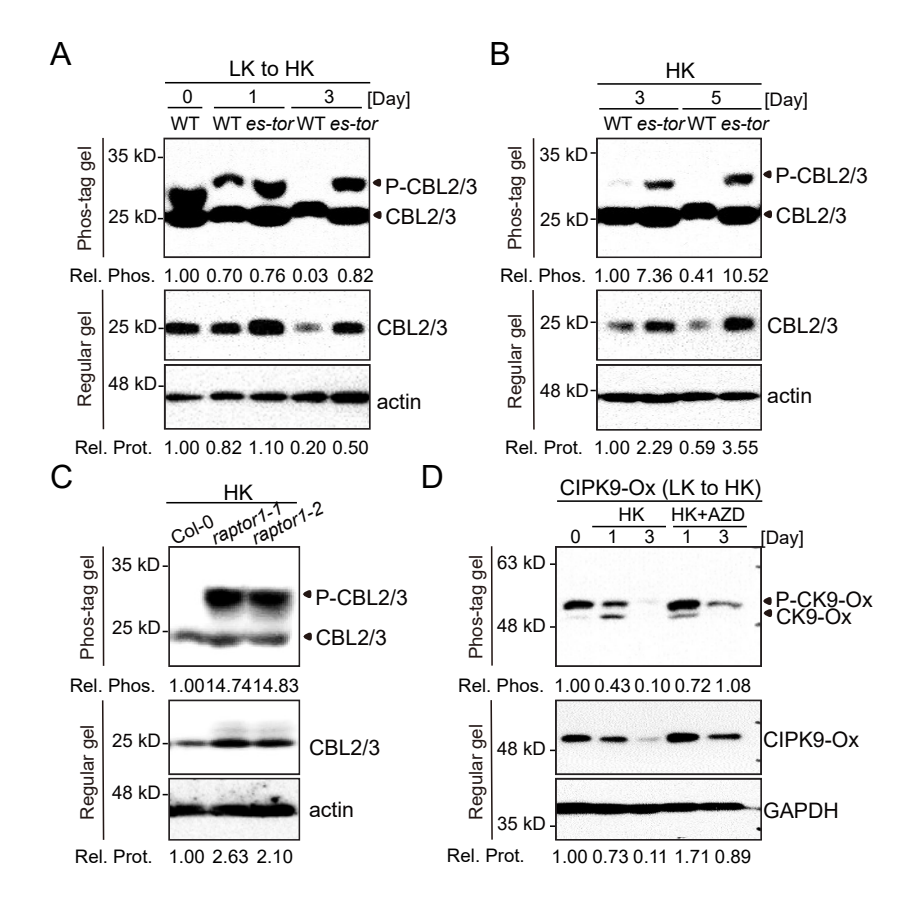


Fig. 3. TORC inhibits CBL2/3-CIPK9 activity. (A) Downregulation of CBL2/3 abundance and phosphorylation upon low-K (LK) to high-K (HK) transfer was blocked by estradiol-induced TOR knockdown. Five-day-old seedlings of es-tor germinated on low-K medium were transferred to the high-K medium without or with 10 μM estradiol for 1 or 3 d. (B) CBL2/3 protein abundance and phosphorylation level increased after TOR knockdown even under a high level of K supply. es-tor seedlings were grown under high-K for 4 d and transferred to high-K medium without or with 10 µM estradiol, for the indicated time, (C) The phosphorylation status and protein level of CBL2/3 in Col and raptor1b mutants grown under high-K for 5 d. (D) High-K-induced dephosphorylation and degradation of CIPK9 was reduced by TOR inhibitor AZD8055. UBQ10: CIPK9-3flag seedlings were grown under low-K for 5 d and transferred to high-K in the presence or absence of 1 μ M AZD8055 for the indicated time. From (A-D), total protein samples were subjected to regular PAGE and phos-tag-PAGE analyses, followed by immunoblot with anti-CBL3 (A-C) or anti-flag (D) antibody. Actin (A-C) or GAPDH (D) was measured in parallel as a loading control. Relative phosphorylation level (Rel. Phos.) was calculated by normalizing phosphorylated against total proteins on "Phos-tag gel." Relative protein level (Rel. Prot.) was calculated by normalizing against actin or GAPDH on "Regular gel." The value of the starting point (0 d) was set to 1. From (A-D), the experiment was repeated three times with similar results.

G548 and S7817 as compared to the wild type. Together, these results suggest that TOR inhibits the activation of the CBL2/3-CIPK module.

In addition to CBL2/3, we next investigated whether TOR is involved in the regulation of CIPK9, a major kinase responsible for CBL2/3 phosphorylation in plant response to low-K stress (19). In the wild-type plants transferred from low- to high-K condition, CIPK9 was dephosphorylated and degraded (Fig. 3D), consistent with the finding in our previous study (19). In contrast, addition of TOR kinase inhibitor AZD8055 to the high-K medium strongly inhibited CIPK9 dephosphorylation and degradation (Fig. 3D). These data supported the conclusion that TORC activation is required for the inactivation of CBL-CIPK signaling during low- to high-K transition.

If TORC inhibits CBL2/3-CIPK9 activity (Fig. 3), it may negatively impact plant response and adaptation to low-K stress. We examined raptor1b mutants, raptor1-1 and raptor1-2, under a low-K condition and found that they displayed an opposite phenotype to the cbl2/3 double mutant. Specifically, low-K treatment more severely inhibited root growth of the cbl2/3 mutant than the effect on the wild type (Fig. 4 A-C). In contrast, two raptor1b mutants showed reduced sensitivity to low-K stress as compared to the wild type grown on MS-agarose plates with or without 1% sucrose (Fig. 4 A–C and SI Appendix, Fig. S5). To further address the role of RAPTOR1B in low-K stress during an extended growth period, we cultured the seedlings hydroponically and examined their phenotypes for 4 weeks. As shown in Fig. 4 D and E, under the high-K condition, the raptor1-2 mutant grew similarly to the wild type, although the *raptor1-1* mutant was slightly smaller than the wild type. When grown in the low-K solution (10 µM), the two raptor 1b mutants both grew significantly better and exhibited longer roots than wild-type plants (Fig. 4 D and E and SI Appendix, Fig. S6), suggesting that RAPTOR1B serves as a negative regulator of plant adaptation to low-K stress. Furthermore, we generated cbl2/3raptor1-2 triple mutants and found that the low-K tolerant phenotype shown in raptor1-2 mutants was abolished in the absence of CBL2/3 (SI Appendix, Fig. S7). These results, coupled with our biochemical results shown in Fig. 3, suggested that the low-K tolerant phenotype in the raptor1 mutant is attributed to increased CBL2/3-CIPK9 activity.

To further assess the function of TOR in plant response to low-K stress, we evaluated the growth of two TOR-overexpressing

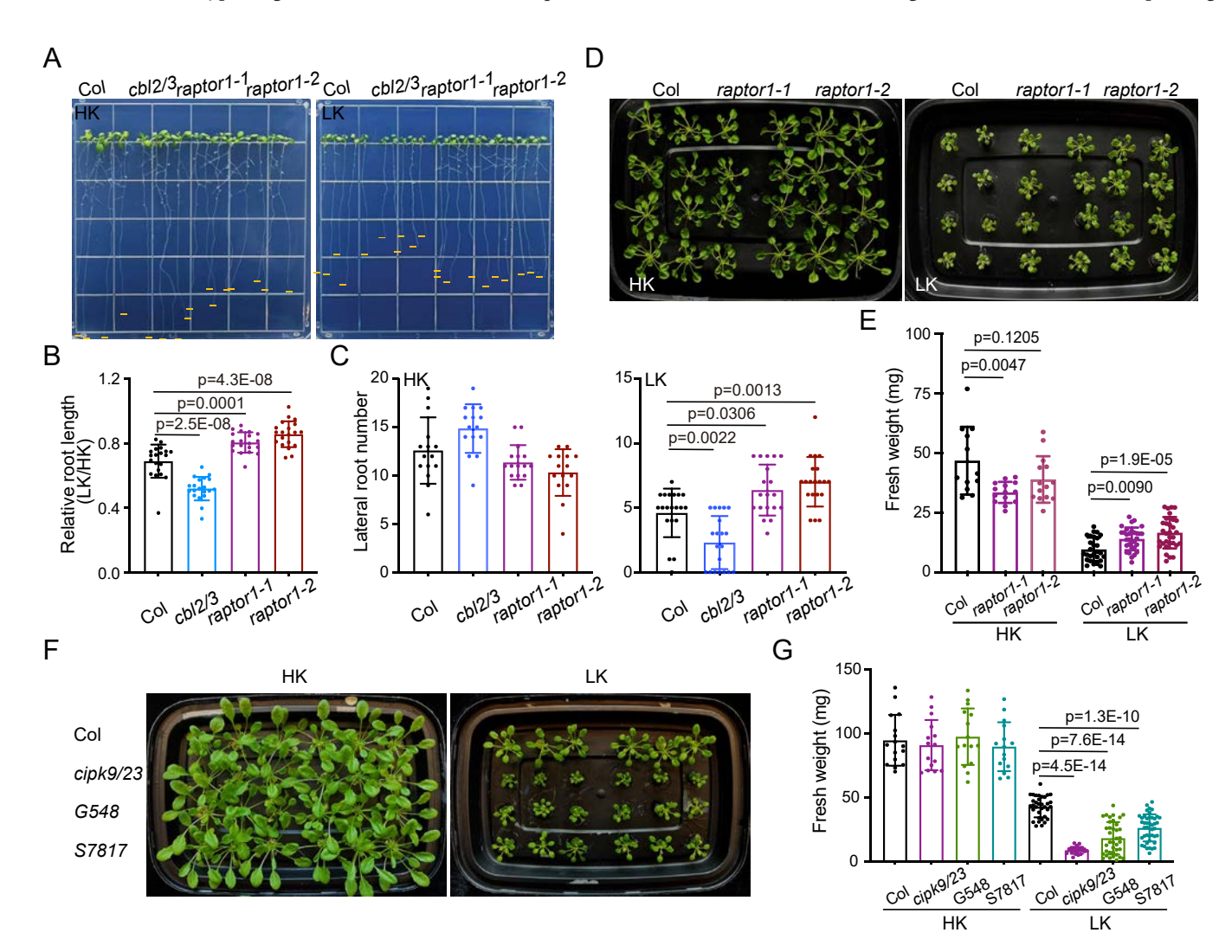


Fig. 4. TORC has a negative impact on low-K tolerance. (A) Representative photos of the wild type (Col), cbl2/3 double mutant, and raptor1b mutants under high- or low-K in post-germination assays. (B) Relative root length was presented as the ratio of root lengths at low K (LK) vs. high-K (HK) condition (as in A). (C) Lateral root number calculated from plants shown in (A). (D) Growth phenotype of 5-week-old wild type and raptor 1b mutants in hydroponic solutions containing high- or low-K. (E) Fresh weight measured at the end of the assay shown in (D). (F) Growth phenotype of 6-week-old plants of wild type, cipk9/23 double mutant, and TOR-Ox lines (G548 and S7817) in high- or low-K hydroponic solutions. (G) Fresh weight measured at the end of the assay shown in (F). Quantitative data in (B, C, E and G) are mean ± SD of at least three biological replicates (n ≥ 12 seedlings). Statistical analyses between groups were performed by one-way ANOVA followed by Tukey's multiple comparison test.

lines (oxTOR lines 7817 and G548) (46) under low-K stress. The TOR-Ox seedlings were hypersensitive to the low-K condition as indicated by shorter roots than the wild type (SI Appendix, Fig. S8). In the hydroponic solutions containing low K (10 μ M), the TOR-Ox plants were more stunted as compared to the wild type, albeit not as severe as the cipk9/23 double mutant (Fig. 4 F and G). Taken together, these data suggest that the TORC pathway negatively regulates the CBL2/3–CIPK9 module that enables low-K adaptation.

CBL-CIPK Represses TORC through Phosphorylating RAPTOR1B.

During low- to high-K transition, TORC is activated and CBL–CIPK is inhibited. We showed above that TORC activation is required for inactivation of the CBL–CIPK activity (Fig. 3), demonstrating one of crosstalk mechanisms between the TORC and the calcium sensor kinase signaling pathways. In response to low-K, CBL–CIPK is activated and TORC is inactivated. We hypothesized that CBL–CIPK may initiate the nutrient deficiency

response and shut down the growth response involving TORC. Thus, inhibition of TORC by CBL-CIPK may serve as the other mechanism for crosstalk between these two signaling pathways. In this context, we proposed a parallel with previous studies in which SnRK (SUCROSE NON-FERMENTING-1-RELATED PROTEIN KINASE) family members, SnRK1/AMPK1, SnRK2, inhibit TORC activity through interacting and phosphorylating RAPTOR1B (47–49). Because CIPKs also belong to the SnRK superfamily and are known as SnRK3 kinases (50), they too may negatively regulate TORC activity by phosphorylating RAPTOR1B. To test this hypothesis, we first tested the physical interactions between RAPTOR1B and CIPK3/9/23/26, respectively, in the yeast two-hybrid system and found that CIPK3/9/26, but not CIPK23, interacted with RAPTOR1B (SI Appendix, Fig. S9). To further confirm the interactions between CIPKs and RAPTOR1B, we used CIPK9 as a representative kinase to perform an in vitro pull-down assay. As shown in Fig. 5 A and B, the GST (glutathione S-transferase)-tagged CIPK9 but not GST pulled down MBP

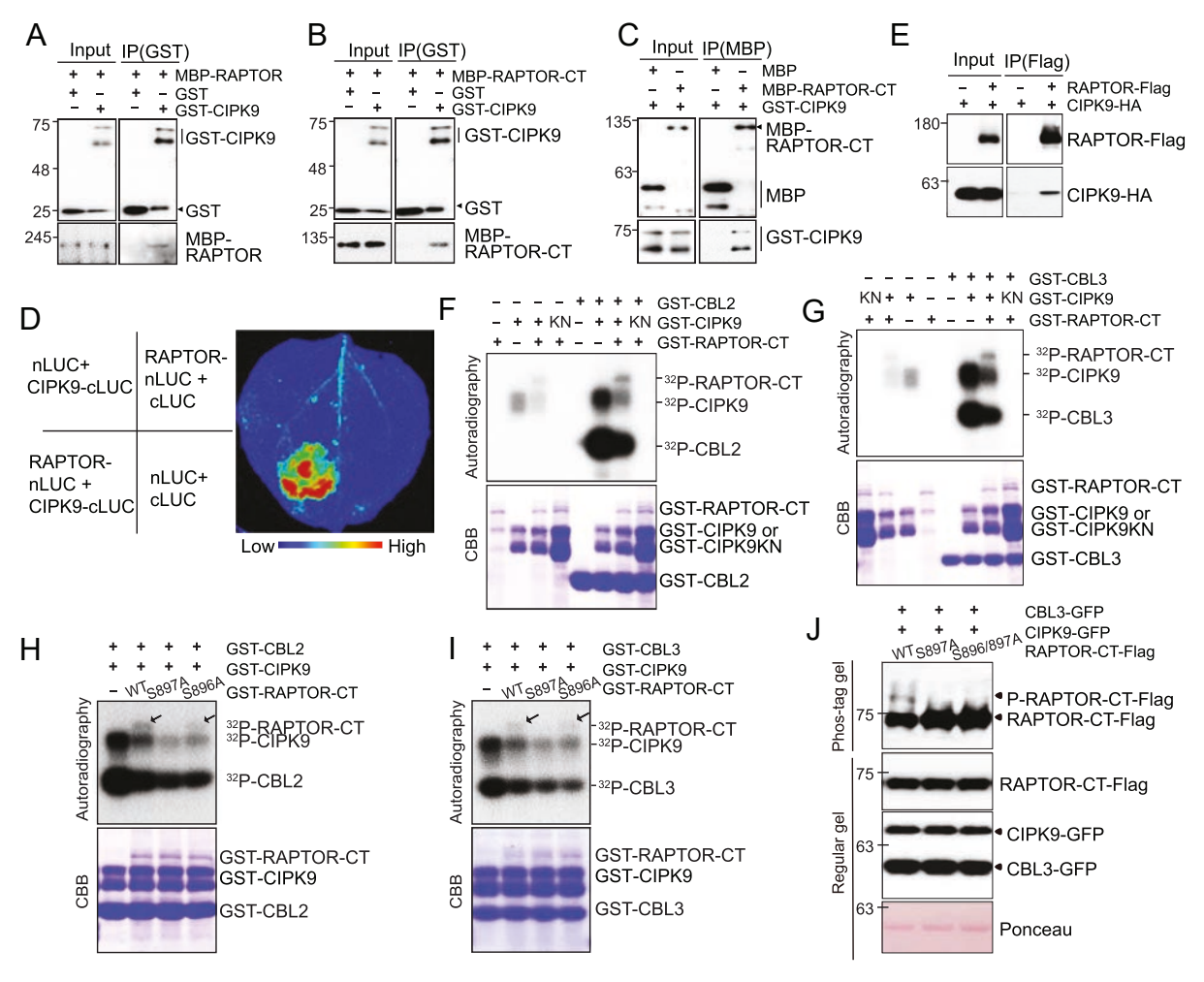


Fig. 5. CIPK9 interacts with and phosphorylates RAPTOR1B at Ser897. (*A*) Interaction between GST-CIPK9 and MBP-RAPTOR1B detected by the pull-down assay. MBP-RAPTOR1B was incubated with GST or GST-CIPK9 and precipitated fractions were analyzed by immunoblots with MBP and GST antibodies. (*B* and *C*) Interaction between GST-CIPK9 and MBP-RAPTOR1B fragment (487 to 1,057 amino acids) analyzed by immunoblots described in (*A*). In (*B*), MBP-RAPTOR1B fragment (487 to 1,057 amino acids) was used as a bait (bound to amylose beads) to pull down GST or GST-CIPK9. In (*C*), GST-CIPK9 was used as a bait (bound to glutathione beads) to pull down MBP or MBP-RAPTOR1B fragment (487 to 1,057 amino acids). (*D*) The interaction between RAPTOR1B and CIPK9 in *N. benthamiana* leaves. RAPTOR1B and CIPK9 proteins were fused to the N- and C-terminal domains of luciferase, respectively, and expressed in *N. benthamiana* leaves. (*C*) Co-IP assay showing interaction between RAPTOR and CIPK9 in *Arabidopsis* cells. CIPK9-HA was expressed alone or coexpressed with RAPTOR1B-Flag in protoplasts. Proteins co-immunoprecipitated by Flag-M2 beads were subjected to immunoblotting using anti-Flag and anti-HA antibodies. (*F* and *G*) Phosphorylation of RAPTOR1B fragments by CBL2/3-CIPK9. (*H* and *I*) Phosphorylation of RAPTOR1B or its mutated versions containing S897A or S896A mutation by CBL2/3-CIPK9. From (*F*-*I*), Phosphorylated proteins were separated by SDS-PAGE and detected by autoradiography (*Upper*). Total proteins loaded to gels were quantified by Coomassie Blue staining (*Bottom*). (*I*) S897A or S896A897A mutations abolished CBL3-CIPK9-induced phosphorylation of RAPTOR1B-CT in *Arabidopsis* protoplasts. Expression levels of RAPTOR1B-CT-Flag, CIPK9-GFP, and CBL3-GFP are shown in Regular gel. Sample loading was monitored by Ponceau S staining of immunoblotting membranes. The experiments were repeated three times, and one representative image is shown.

(maltose-binding protein)-tagged full-length RAPTOR1B or a C-terminal region of RAPTOR1B (487-1057 aa). Furthermore, MBP-tagged RAPTOR1B fragment (487-1057 aa), but not MBP, pulled down GST-CIPK9 (Fig. 5C). To test whether the interaction between RAPTOR1B and CIPK9 occurs in plant cells, we performed the firefly luciferase complementation imaging assay in Nicotiana benthamiana leaves and observed strong luciferase activity specifically when RAPTOR1B and CIPK9 were coexpressed (Fig. 5D), indicating a direct interaction between RAPTOR1B and CIPK9 in plants. Additionally, we also performed a co-immunoprecipitation (co-IP) assay in Arabidopsis protoplasts (Fig. 5*E*), which further confirmed this interaction.

We next tested whether CIPK9, like SnRK1 and SnRK2 kinases, phosphorylates RAPTOR1B using an in vitro kinase assay. As shown in Fig. 5 F and G, the recombinant CIPK9, but not the dead kinase CIPK9K48N, showed autophosphorylation activity and phosphorylated CBL2 and CBL3, and the kinase activity of CIPK9 was enhanced by CBL2 or CBL3, which are consistent with previous findings (19, 51). Importantly, CBL2 or CBL3 together with CIPK9 phosphorylated RAPTOR1B fragment (487–1057 aa) (Fig. 5 F and G and SI Appendix, Fig. S10), identifying RAPTOR1B as a direct substrate of CIPK9. Interestingly, the inclusion of RAPTOR1B repressed CIPK9 autophosphorylation and transphosphorylation activity against CBL2/3 (Fig. 5 F and G and SI Appendix, Fig. S10), consistent with our finding that TOR-RAPTOR1B negatively regulates CBL2/3-CIPK9 action in plants (Fig. 3). Furthermore, we performed an in vivo phosphorylation assay using Arabidopsis protoplasts. As shown in SI Appendix, Fig. S11, RAPTOR1B-CT-Flag proteins became up-shifted in the Phos-tag gel upon coexpression of CBL3-CIPK9. Phosphatase treatment removed this mobility shift, indicating that the upper band was the phosphorylated form of RAPTOR1B-CT protein.

To map the CIPK9-mediated phosphorylation site(s) on RAPTOR1B, we performed an in vitro kinase assay coupled with LC-MS/MS analysis. The MS spectra revealed only one phosphorylation modification at either Serine896 or Serine897 of RAPTOR1B (487–1057 aa) fragment (SI Appendix, Fig. S12). Subsequently, we found that a Ser-to-Ala substitution at Ser897, but not Ser-to-Ala substitution at Ser896, substantially reduced the phosphorylation by CBL2-CIPK9 or CBL3-CIPK9 when compared to the wild-type RAPTOR1B fragment (Fig. 5 H and I and SI Appendix, Fig. S13). Moreover, either S897A or S896A897A mutation abolished CBL3-CIPK9-induced phosphorylation of RAPTOR1B-CT in *Arabidopsis* protoplasts (Fig. 5/). These results together suggested that Ser897 is the major phosphorylation site for CIPK9.

It has been shown that the phosphorylation of RAPTOR1B-Ser897 by SnRK2 results in disassociation of RAPTOR1B from the TORC and inhibits TOR kinase activity (49). We thus conclude that CBL2/3–CIPK9 represses TORC activity through phosphorylating Ser897 of RAPTOR1B. In support of this conclusion, we found that expression of CBL2-CIPK9 or CBL3-CIPK9 in Arabidopsis protoplast assays effectively suppressed S6K1-pT449 phosphorylation, suggesting that CBL2/3-CIPK9 modules effectively inhibit TORC activity (SI Appendix, Fig. S14). If CBL-CIPK negatively regulates TORC activity, reducing CBL-CIPK activity in plants would render plants less sensitive to TORC inhibitors. We thus measured the sensitivity to AZD8055 in cbl2/3, cipk9, and raptor1b mutants. Our results showed that the raptor1b mutant was hypersensitive, whereas cbl2/3 and cipk9 mutants were less sensitive to AZD8055-mediated growth inhibition when compared to the wild type (SI Appendix, Fig. S15). The opposite pattern of AZD8055 sensitivity observed in cbl2/3-cipk9 versus raptor1b mutants further

supported the conclusion that CBL2/3-CIPK9 is a negative regulator of TORC activity.

If CBL2/3-CIPK9 inhibits TORC activity, turning off CBL-CIPK network may expedite plant recovery once low-K stress subsides. We examined growth recovery of cbl2/3, cipk9 as well as raptor1b mutant during low- to high-K transfer. As shown in Fig. 6 A and B, the raptorb1b mutant exhibited significant growth retardation as compared with the wild type in response to K repletion treatment, consistent with our finding that TORC is indispensable for high-K promoted growth (Fig.1 A-F). Interestingly, although cbl2/3 and cipk9 mutants showed severe growth defects when grown on medium containing low-K, upon transfer to medium containing high-K, cbl2/3 and cipk9 mutants displayed more rapid recovery from low-K stress as compared to the wild type (Fig. 6 A and B). Furthermore, the faster growth recovery in cbl2/3 and cipk9 mutants was completely abolished by the addition of 2 μM AZD8055 to the high-K medium (Fig. 6C). These results again supported the conclusion that CBL2/3-CIPK9 negatively regulates TORC activity in plant responses to K repletion.

Discussion

Mineral nutrient availability is an important external signal for plants to respond and adapt to in order to survive and thrive. Although K⁺ is the most abundant mineral in plants, mechanisms underlying K sensing and response remain unclear. In this study, we have shown that TORC activity is essential for high-K-mediated plant growth, and its activity is fine-tuned by external K levels: K deprivation represses TOR activity, while K repletion rapidly reactivates TORC (Figs. 1 and 2). Once activated by sufficient K, TORC serves as a molecular switch that shuts down K-deficiency response mediated by a Ca-dependent CBL-CIPK network. In response to K-deficiency, the CBL-CIPK pathway dominates, leading to inhibition of TORC and growth arrest to conserve energy and ensure survival. The crosstalk between TORC and CBL2/3-CIPK9 network is therefore a critical mechanism by which plants switch between growth and adaptation modes in response to changing K nutrient status (Fig. 6D).

Several findings from this study add significantly to our understanding of nutrient sensing in plants, including the identification of the link between K response and TORC activation. The TORC is a highly conserved master regulator that integrates nutrients, hormones, and stress signals to control cell proliferation and growth in all eukaryotes (22, 32, 34, 37, 52). In the context of nutrient sensing, TORC activity is highly regulated by nutrient availability especially organic compounds such as sugars, amino acids, and nucleotides (23, 32, 33). In plants, TORC is not only responsive to organic nutrients but also inorganic nutrients including nitrogen salts, phosphate, and sulfate (22, 34-38, 53, 54). As the most abundant mineral in plant cells, K⁺ is a unique nutrient in that it remains in the ionic form without being metabolized into organic forms. In all eukaryotes including mammals, fungi, and plants, it is unknown how K+ is sensed and whether TORC is involved in response to changing K status. One study indicates that K-deficiency, instead of sufficient K, appears to slightly activate TORC1 in yeast (55) although functional relevance of this observation is not examined. Our study here demonstrates that high external K rapidly activates and K-deficiency inhibits TORC in Arabidopsis (Fig. 2). Consistently, TORC is required for K-dependent plant growth, placing TORC in between K nutrient sensing and plant growth (Fig. 1). Once TORC is activated, it switches off the low-K stress response network that consists of CBL2/3-CIPK9 signaling modules. TORC-mediated regulation of the CBL-CIPK pathway was strongly supported by several

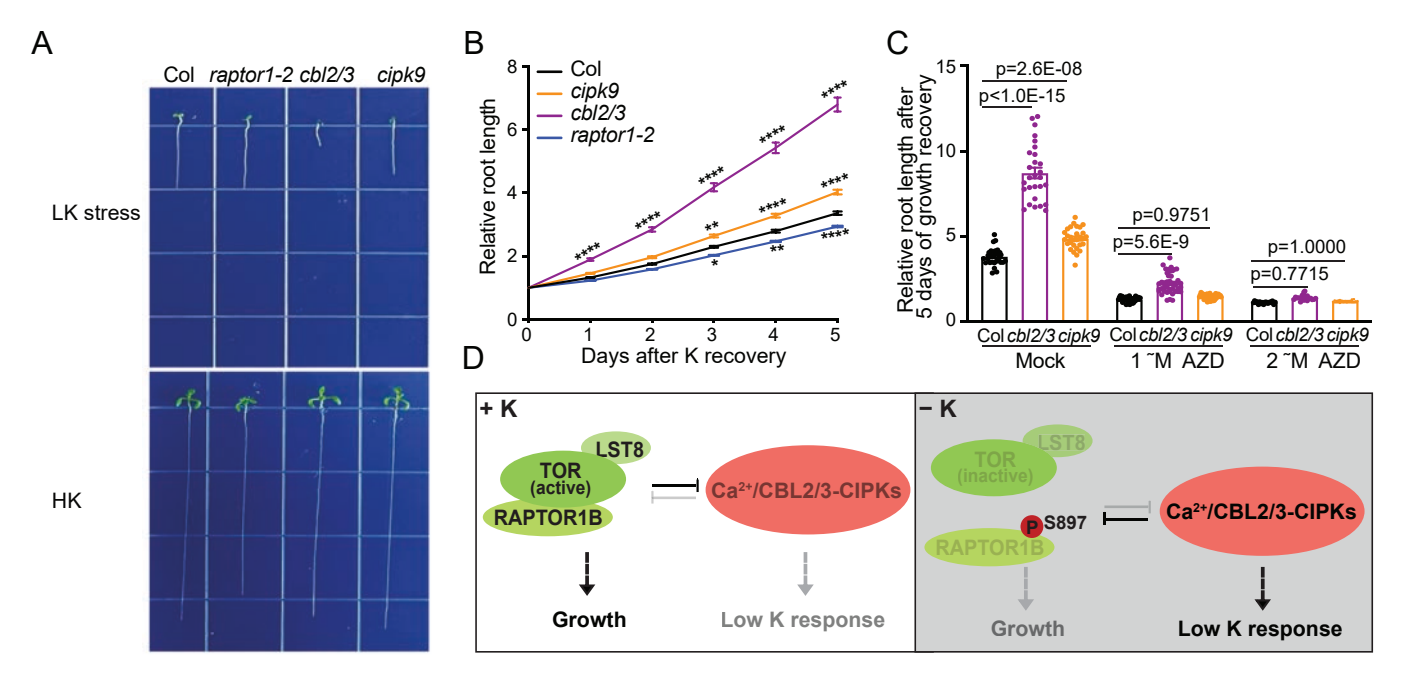


Fig. 6. CBL2/3–CIPK9 negatively regulates TORC activity in response to K repletion. (*A*) Representative images of wild type (Col), *raptor1b*, *cbl2/3*, and *cipk9* mutants before and after 5 d of growth on K repletion medium. The seedlings were grown on low-K medium for 5 d and then were transferred to high-K medium for 5 d before taking photos. (*B*) Relative root length of seedlings was measured at different time points after transfer to high-K medium. The value of the starting point (day 0) was set to 1. (C) Relative root length of wild type (Col), *cbl2/3*, and *cipk9* seedlings after 5 d of growth on high-K or high-K plus AZD8055 medium. Seeds of Col, *cbl2/3*, and *cipk9* were germinated and grown on low-K medium for 5 d before transferred to high-K medium without or with 1 μM or 2 μM AZD8055 for 5 d. Quantitative data in (*B* and *C*) are mean ± SEM of three biological replicates ($n \ge 34$ seedlings in *B*, $n \ge 18$ seedlings in *C*). Statistical analyses between groups were performed by two-way ANOVA followed by Tukey's multiple comparison test. In (*B*), *P < 0.05, **P < 0.01, ****P < 0.001. (*D*) Working model for TORC and CBL–CIPK signaling pathways to orchestrate growth and low-K response under changing K status. When K is sufficient, TORC rapidly activates to turn off the CBL–CIPK-mediated low-K response network and promotes plant growth. In response to K deficiency, the CBL–CIPK pathway dominates, inactivating TORC by phosphorylating RAPTOR1B and slowing down the growth to switch to adaptation mode.

pieces of evidence including 1) elevated CBL-CIPK activity after inducible knockdown of TOR in the es-tor plants, 2) elevated CBL-CIPK activity in *raptor1b* mutants, 3) elevated CBL-CIPK activity in plants treated with TOR inhibitors, 4) improved low-K tolerance in raptor1b mutants, and 5) lower levels of CBL-CIPK activity and impaired low-K tolerance in TOR-overexpressing lines (Figs. 3 and 4 and SI Appendix, Figs. S1-S8). However, the mechanistic process by which TORC represses the CBL-CIPK pathway remains largely unknown. Our initial work suggested that TORC may inhibit the kinase activity of CIPKs, at least in part, through direct interaction of RAPTOR with CIPKs. Such interaction may allow TORC to enhance CIPK9 autoinhibition, which was supported by the observation that RAPTOR1B represses CIPK9 autophosphorylation even in the absence of CBL2/3 (Fig. 5 F and *G*). The second possibility is that RAPTOR1B-CIPK9 interaction may interrupt or compete with CBL2/3-CIPK9 interaction. The third is through manipulating intracellular K levels as TORC inhibitors have been shown to cause a decrease of K contents in yeast and plants although the mechanism is unclear (55, 56). Finally, we cannot exclude the possibility that TORC may phosphorylate and regulate unknown factor(s) that in turn control CBL2/3-CIPK9 protein stability and phosphorylation status. Future work is thus expected to resolve these possibilities and to identify the detailed mechanistic process by which TORC shuts down the low-K response network in plants. Another line of future research should be to fill the gap between K nutrient sensing and TORC activation. While TORC activation is an early event (within 30' after low- to high-K transfer) in the K-sensing pathway, the underlying mechanism whereby elevated K nutrient status activates TORC remains to be uncovered. It has been reported that glucose can rapidly activate TOR through mitochondria-based energy metabolism (22). Given that K is highly relevant to carbon

metabolism and mitochondrial function, it is plausible that TORC senses K indirectly through glucose or energy status in plant cells. In addition, the small GTPase ROP2 has been shown to mediate TORC activation by auxin (45, 57, 58). Interestingly, IAA levels and distribution in *Arabidopsis* roots can vary under changing external K levels (8, 59–61). This raises the possibility of crosstalk between K status and auxin-ROP GTPase nexus. Exploring these possibilities in further investigations will be essential to unravel the intricate mechanism by which plant TORC senses and responds to K levels in the soil.

In addition to TORC-mediated shutdown of the CBL-CIPK pathway, we also revealed inhibition of TORC activity by CBL-CIPK in response to low-K stress conditions. In this regard, it has been shown that multiple protein kinases down-regulate TORC function by phosphorylating RAPTOR especially under stress conditions (47-50, 62, 63). For example, both AMPK/SnRK1s and SnRK2s inhibit TORC signaling through phosphorylating RAPTOR/RAPTOR1B (47-49). In this study, we found that CIPK9 directly interacted with RAPTOR1B and phosphorylated the Ser897 in RAPTOR1B (Fig.5 and SI Appendix, Figs. S9–S13), which represents a conserved mechanism for TORC regulation by kinases in the SnRK superfamily. Thus, inhibition of TORC activity by SnRK1s, SnRK2s, and CIPKs, which are all activated upon stress conditions (e.g., intracellular low energy for SnRK1, abiotic stress for SnRK2, and low-nutrient status for CIPKs), may switch to survival/adaptation mode by repressing plant growth through down-regulation of TORC. There are 10 CBLs and 26 CIPKs in Arabidopsis and the large number of Ca2+-CBLs-CIPKs modules have been shown to function broadly in the responses to various stress conditions beyond K deficiency (64). It will be important to investigate how CBL-CIPK modules are involved in the regulation of TORC signaling under other stress conditions.

Materials and Methods

Plant Materials and Growth Conditions. All the wild-type, mutant, and transgenic Arabidopsis lines used in this study are Columbia (Col-0) ecotype. Detailed information on T-DNA insertion mutants used in this study is as follows: cbl2/3(cbl2cbl3) (18), cipk9/23 (cipk9cikp23) (18), raptor1-1 (SALK_078159)(41), raptor1-2 (SALK_006431) (41), es-tor (40), S7817 (46), G548 (46), and UBQ10: CIPK9-3flag/cipk9cipk23 (19). The cbl2cbl3raptor1b triple mutant was generated through genetic across, and the homozygous mutant plants were subsequently identified from the F₃ progeny using PCR-based genotyping. All the primers used for genotyping are listed in SI Appendix, Table S1.

Growth Conditions for Arabidopsis Seedlings under Different K Regimes. All seeds were surface sterilized with 10% bleach for 15 min, washed three times with water, and sown on the growth medium solidified with 0.8% (w/v) BD BBLTM select agar. The recipe of the growth medium was modified from MS medium with a reduced level of NH₄⁺, which contained the following components: 3 mM $Ca(NO_3)_2$, 1.25 mM $NH_4H_2PO_4$, 1.5 mM $MgSO_4$, 1 × Murashige, and Skoog (MS) micronutrients (contain 5 µM K), and 1% (w/v) sucrose. The pH of the medium was adjusted to 5.8 using NaOH. The final K concentration in the medium was adjusted by adding KCl as the K source. K⁺ concentrations in high-K and low-K medium are 10 mM and 10 µM, respectively, unless indicated otherwise.

For the germination phenotyping assay, seedlings were germinated on modified MS medium shown above with different concentrations of K and incubated at 4 °C for 2 d for stratification, then were transferred to a growth chamber with 120 $\mu mol\ m^{-2}\ s^{-1}$ light intensity with a 12-h light/12-h dark photoperiod for the indicated days.

For the post-germination phenotyping assay, seeds were germinated on modified MS medium containing high-K (10 mM) and grown for 4 d. The seedlings were then transferred onto various agarose-solidified modified MS medium [3 mM Ca (NO₃)₂, 1.25 mM NH₄H₂PO₄, 1.5 mM MgSO₄, 1 \times Murashige and Skoog (MS) micronutrients, and 1% (w/v) sucrose, pH 5.8] supplemented with different concentrations of K for subsequent growth under 120 µmol m⁻² s⁻¹ light intensity with a 12-h light/12-h dark photoperiod. At the end of the assay, the root length of seedlings was measured by ImageJ software.

For the phenotypic assay in the hydroponics, seeds were germinated on MS medium and grown for 7 d. The seedlings were then transferred to the liquid solution containing 1.4 mM Ca(NO₃)₂, 0.1 mM Ca(H₂PO₄)₂, 0.125 mM MgSO₄, and 0.025 mM MgCl₂, as well as 1/6 strength of MS minor salts and supplemented with different concentrations of KCl. All the hydroponic solutions for plant growth were replaced with fresh ones twice a week.

RNA Isolation and Quantitative Real-time PCR Analysis. Total RNA was extracted from plant samples using the TRIZOL reagent (Invitrogen). After being treated with DNase I (Invitrogen) to remove DNA contamination, cDNA was synthesized using the SuperScript II reverse transcriptase kit (Invitrogen). The quantitative real-time PCR analysis was performed on the DNA Engine Opticon System (MJ Research) using the SYBR Green Realtime PCR Master Mix (Bio-Rad). All experiments were performed using three biological replicates, and Actin served as an internal standard. The relative expression of each gene was calculated using the $\Delta\Delta$ CT method (2^{- $\Delta\Delta$ CT}) (65). Each experiment was repeated with three different batches of samples and RT-PCR reactions were performed with three technical replicates for each sample. The primers used in quantitative real-time PCR are listed in *SI Appendix*, Table S1.

Assays for TORC Activity in Seedlings under Varying K Levels. To prepare seedlings for K deficiency assays, 35S:S6K1-HA seeds were germinated and cultured on the modified MS medium containing 2 mM K for 8 d before the seedlings were transferred to the modified MS medium containing 2 mM K or 10 μ M K for the indicated time. The seedlings on the 2 mM K medium served as controls.

To prepare seedlings for K repletion assays, 35S:S6K1-HA seeds were germinated and grown on the modified MS medium containing 10 μ M K for 8 d before the seedlings were transferred to the modified MS liquid medium containing elevated K concentrations (for dose-dependent assays) and harvested at various time points (for time course experiments).

Protein Extraction and Immunoblots. For total protein extraction, Arabidopsis seedlings were grounded in the presence of liquid nitrogen to fine powder, and total protein was extracted with 2 × SDS sample buffer (100 mM Tris-Cl, pH6.8,

4% SDS, 0.2% bromophenol blue, 20% glycerol, and freshly added 10% β -mercaptoethanol). Aliquots of denatured total protein were separated by SDS-PAGE and transferred to a PVDF membrane. For the detection of phosphorylated CBL proteins, total protein was separated by 10% SDS-PAGE with 15 µM Phos-tag (AAL-107, WAKO pure chemical industries, Ltd) and transferred to PVDF membrane. For immunoblot analyses, anti-CBL3 (19, 66), anti-GAPDH (PHYTOAB, PHY0303A), anti-actin (PHYTOAB, PHY0001), anti-Flag (Sigma-Aldrich, A8592-2MG), anti-S6K1-p (phosphor T449) (Abcam, ab207399), anti-HA (Santa Cruz Biotechnology, sc-7392HRP) were used as primary antibodies. Each experiment was repeated at least three times, and one representative result is shown in the figures. Band density in immunoblots was quantified using Image J software.

Yeast Two Hybrid Assay. To examine interactions between RAPTOR1B and CIPKs, pGADT7 plasmids containing CIPK9 were co-transformed with pGBKT7-RAPTOR1B into Saccharomyces cerevisiae AH109 cells. Successfully transformed colonies were identified on yeast SD medium lacking Leu and Trp. Colonies were transferred to selective SD medium lacking Leu, Trp, and His as indicated. To determine the intensity of protein interaction, saturated yeast cultures were diluted to 10^{-1} , 10^{-2} , and 10^{-3} and spotted onto the selection medium. Photographs were taken after 4-d incubation at 30 °C. The primers used in generating the yeast constructs are listed in SI Appendix, Table S1.

Pull-Down Assay. The constructs for expressing GST-CBL2, GST-CBL3, and GST-CIPK9 were described previously (19). Full-length RAPTOR1B and RAPTOR1B fragments were inserted into pMal-C2X vector to fuse with maltose-binding protein (MBP) or into pGEX4T-1 vector to fuse with GST. All constructs were transformed into Escherichia coli strain BL21, and protein expression was induced by addition of 1 mM IPTG (isopropyl-β-D-thiogalactopyranoside) to the culture. Two micrograms of MBP, MBP-RAPTOR1B, or MBP-RAPTOR1B-CT was mixed with 2 µg GST or GST-tagged proteins in 500 µL binding buffer (20 mM Tris-HCl, pH 7.5, 150 mM NaCl and 0.1% Nonidet P-40), and the mixture was mixed at 4 °C for 1 h. Amylase agarose beads or GST beads were washed with binding buffer for three times and then added into the mixture. The mixture was rotated at 4 °C for another 1 h. After being washed for five times with binding buffer, the MBP or GST beads were boiled with protein loading buffer and analyzed by immunoblots. Anti-GST (Sigma-Aldrich, Cat. No: G1160-.2ML) at 1:1,000 dilution or anti-MBP (New England Biolabs, Cat. No: E8032S) at 1:1000 dilution was used for the western blots. The primers used in the construction of related vectors and plasmids are listed in SI Appendix, Table S1.

Co-Immunoprecipitation (Co-IP). For Co-IP assays in plant cells, Arabidopsis mesophyll protoplasts were co-transfected with constructs expressing 3 × Flaq- or 3 × HA-tagged proteins following established protocols as previously described (67). Protoplasts were collected and lysed in IP buffer containing 50 mM HEPES (NaOH, pH 7.5), 150 mM NaCl, 50 mM β-glycerophosphate, 2 mM DTT, 1% Triton X-100 and 10% glycerol, EDTA-free protease inhibitor (Roche), and Phostop phosphatase inhibitor (Roche). A 40- μ L aliquot of the lysate was used as the input. The remaining lysate was incubated with 10 μ L of prewashed anti-Flag M2 agarose beads (Sigma-Aldrich) on a roller shaker for 1 h at 4 °C. The beads were then washed three times with IP buffer, and bound proteins were eluted by boiling in 1 × SDS-PAGE loading buffer. Input and IP fractions were immunoblotted with HRP-conjugated anti-Flag or HRP-conjugated anti-HA antibodies, respectively. The primers used in the construction of related plasmids are listed in SI Appendix, Table S1.

In Vivo Phosphorylation. For in vivo phosphorylation, protoplast isolation and DNA transfection were performed as described previously (67). After transfection with the plasmids and a subsequent 12-h incubation at room temperature to enable protein expression, cells were collected, and proteins were extracted using the IP buffer as described above for the Co-IP assay. Total protein samples were separated on a Phos-tag acrylamide gel (25 μM, Wako Chemicals). Immunoblotting analysis was performed using HRP-conjugated anti-Flag or HRP-conjugated anti-HA antibodies.

For the dephosphorylation of RAPTOR1B-CT, 3 × Flag-tagged RAPTOR1B-CT protein was isolated using an extraction buffer containing 50 mM HEPES (NaOH, pH 7.5), 150 mM NaCl, 2 mM DTT, 0.5% Triton X-100, and 10% glycerol, supplemented with EDTA-free protease inhibitor (Roche). After centrifugation at 15,000 g for 10 min, the supernatant was incubated with 10 μ L prewashed anti-Flag M2 agarose beads for 1 h at 4 °C on a roller shaker. The beads were washed twice with the extraction buffer and once with $1 \times dephosphoryla$ tion buffer provided in a lambda protein phosphatase package (λ -PPase, New England Biolabs). The protein-bound beads were then directly used for phosphatase reactions following the manufacturer's instructions. Proteins were eluted using 1 × SDS-PAGE loading buffer and boiled for 5 min before being separated on a Phos-tag gel.

Firefly Luciferase Complementation Imaging Assay. The CIPK9-cLUC plasmid was described previously (68). The coding sequence of RAPTOR1B was in-frame fused with the N-terminal region of the luciferase protein sequence under the control of the 35S promoter. The constructs for protein expression were transformed into the Agrobacterium tumefaciens GV3101 strain. For plant transient expression, different combinations of Agrobacterium transformants carrying various constructs were co-infiltrated into the leaves of *Nicotiana benthamiana* in the presence of p19, a viral gene silencing suppressor. Two days after infiltration, leaves infiltrated with split-luciferase complementation constructs were sprayed with 1 mM D-luciferin (Neta Scientific), and the luciferase activities were detected by a BioRad CCD imaging system. The primers used in related constructs are listed in *SI Appendix*, Table S1.

In Vitro Kinase Assay. The coding sequences of CIPK9, CBL2, CBL3, and RAPTOR1B were cloned in pGEX4T-1 vector and expressed in E. coli as a GST (glutathione S-transferase) fusion proteins (19) (SI Appendix, Table S1). All

- Y. Wang, W. H. Wu, Potassium transport and signaling in higher plants. Annu. Rev. Plant Biol. 64, 451-476 (2013).
- D. P. Schachtman, R. Shin, Nutrient sensing and signaling: NPKS. Annu. Rev. Plant Biol. 58, 47-69 (2007).
- W. T. Pettigrew, Potassium influences on yield and quality production for maize, wheat, soybean and cotton. Physiol. Plant 133, 670-681 (2008).
- A. Amtmann, P. Armengaud, The role of calcium sensor-interacting protein kinases in plant adaptation to potassium-deficiency: New answers to old questions. Cell Res. 17, 483-485 (2007)
- C. Zorb, M. Senbayram, E. Peiter, Potassium in agriculture-status and perspectives. J. Plant Physiol. **171**, 656-669 (2014).
- A. K. Srivastava et al., Emerging concepts of potassium homeostasis in plants. J. Exp. Bot. 71, 608-619 (2020).
- Chandini, R. Kumar, R. Kumar, O. Prakash, "The impact of chemical fertilizers on our environment and ecosystem" in Research Trends in Environmental Sciences, P. Sharma, Eds. (Scientific Research, New Delhi: AkiNik Publications, 2019), vol. 5, pp. 69-86.
- Y. Wang, Y. F. Chen, W. H. Wu, Potassium and phosphorus transport and signaling in plants. J. Integr. Plant Biol. 63, 34-52 (2021).
- D. J. Walker, R. A. Leigh, A. J. Miller, Potassium homeostasis in vacuolate plant cells. Proc. Natl. Acad. Sci. U.S.A. 93, 10510-10514 (1996).
- M. K. Ashley, M. Grant, A. Grabov, Plant responses to potassium deficiencies: A role for potassium transport proteins. J. Exp. Bot. 57, 425-436 (2006).
- 11. Connections through the CBL-CIPK Network, S. Luan, W. Lan, S. Chul Lee, Potassium nutrition, sodium toxicity, and calcium signaling. Curr. Opin. Plant Biol. 12, 339-346 (2009).
- F. J. Maathuis, Physiological functions of mineral macronutrients. Curr. Opin. Plant Biol. 12, 250-258 (2009).
- J. Xu *et al.*, A protein kinase, interacting with two calcineurin B-like proteins, regulates K+ transporter AKT1 in Arabidopsis. *Cell* **125**, 1347–1360 (2006). L. Li, B. G. Kim, Y. H. Cheong, G. K. Pandey, S. Luan, A Ca(2)+ signaling pathway regulates a K(+)
- channel for low-K response in Arabidopsis Proc. Natl. Acad. Sci. U.S.A. 103, 12625-12630 (2006). P. Ragel et al., The CBL-interacting protein kinase CIPK23 regulates HAK5-mediated high-affinity K+ uptake in Arabidopsis roots. Plant Physiol. 169, 2863-2873 (2015).
- A. Lara et al., Arabidopsis K+ transporter HAK5-mediated high-affinity root K+ uptake is regulated by protein kinases CIPK1 and CIPK9. J. Exp. Bot. 71, 5053-5060 (2020).
- Y. H. Cheong et al., Two calcineurin B-like calcium sensors, interacting with protein kinase CIPK23, regulate leaf transpiration and root potassium uptake in Arabidopsis. Plant J. 52, 223-239 (2007).
- R. J. Tang et al., Author Correction: A calcium signalling network activates vacuolar K(+) remobilization to enable plant adaptation to low-K environments. Nat. Plants 7, 236 (2021).
- K. L. Li, R. J. Tang, C. Wang, S. Luan, Potassium nutrient status drives posttranslational regulation of a low-K response network in Arabidopsis. Nat. Commun. 14, 360 (2023).
- T. Dobrenel et al., TOR signaling and nutrient sensing. Annu. Rev. Plant Biol. 67, 261–285 (2016).
- M. Laplante, D. M. Sabatini, mTOR signaling in growth control and disease. Cell 149, 274-293 (2012)
- Y. Xiong et al., Glucose-TOR signalling reprograms the transcriptome and activates meristems. Nature 496, 181-186 (2013).
- Y. Meng et al., TOR kinase, a GPS in the complex nutrient and hormonal signaling networks to guide plant growth and development. J. Exp. Bot. 73, 7041-7054 (2022).
- L. Fu et al., The TOR-EIN2 axis mediates nuclear signalling to modulate plant growth. Nature 591, 288-292 (2021).
- X. Yuan, P. Xu, Y. Yu, Y. Xiong, Glucose-TOR signaling regulates PIN2 stability to orchestrate auxin gradient and cell expansion in Arabidopsis root. Proc. Natl. Acad. Sci. U.S.A. 117, 32223-32225 (2020).
- K. M. Jamsheer, S. Jindal, A. Laxmi, Evolution of TOR-SnRK dynamics in green plants and its integration with phytohormone signaling networks. J. Exp. Bot. 70, 2239-2259 (2019).
- G. H. Anderson, B. Veit, M. R. Hanson, The Arabidopsis AtRaptor genes are essential for post-embryonic plant growth. BMC Biol. 3, 12 (2005).

MBP- and GST-tagged proteins were purified according to the manufacturer's instructions. For in vitro phosphorylation, 0.5-2.0 µg of purified kinase and substrate proteins was incubated in the kinase reaction buffer containing 20 mM Tris (pH 7.2), 2.5 mM MnCl₂, 0.5 mM CaCl₂, 1 mM DTT, 10 mM ATP, and 2 μ Ci ³²P γ -ATP at 30 °C for 30 min and terminated by adding 5 × SDS-PAGE loading buffer and boiling for 5 min. The samples were analyzed using a 12% SDS-PAGE gel, followed by Coomassie Blue staining and autoradiography. Coomassie staining was used to verify the quality of samples and loading consistency.

Root Lengths Measurement. After the indicated times of growth and treatment, seedlings were laid on the agar plates, and digital pictures were taken. The root lengths were measured using ImageJ software.

Data, Materials, and Software Availability. All study data are included in the article and/or SI Appendix.

ACKNOWLEDGMENTS. We thank Drs. Jen Sheen and Jacob O. Brunkard for sharing 35S:S6K1-HA and raptor1b mutant seeds; Drs. Yan Xiong and Zhiyong Wang for es-tor and TOR-Ox lines S7817 and G548; Dr. Feng Yu for BD-RAPTOR1B plasmid; Dr. Chao Wang for 35S: CIPK9-cLUC, PUC19-CBL2/3-GFP, and PUC19-CIPK9-GFP plasmids, and Dr. Dhondup Lhamo for helpful discussions. This work was supported by grants from the NSF (MCB-1714795, MCB-2041585, and ISO-1339239) and the California Agriculture Experimental Station.

- 28. Y. Xiong, J. Sheen, Novel links in the plant TOR kinase signaling network. Curr. Opin. Plant Biol. 28, 83-91 (2015).
- L. Shi, Y. Wu, J. Sheen, TOR signaling in plants: Conservation and innovation. Development 145, dev160887 (2018).
- 30. M. A. Salem et al., RAPTOR controls developmental growth transitions by altering the hormonal and metabolic balance. Plant Physiol. 177, 565-593 (2018).
- L. Dai et al., The TOR complex controls ATP levels to regulate actin cytoskeleton dynamics in Arabidopsis. Proc. Natl. Acad. Sci. U.S.A. 119, e2122969119 (2022).
- J. Kim, K. L. Guan, mTOR as a central hub of nutrient signalling and cell growth. Nat. Cell Biol. 21, 63-71 (2019).
- R. A. Saxton, D. M. Sabatini, mTOR signaling in growth, metabolism, and disease. Cell 169, 361-371 (2017).
- P. Cao et al., Homeostasis of branched-chain amino acids is critical for the activity of TOR signaling in Arabidopsis. eLlife 8, e50747 (2019).
- L. Fu, P. Wang, Y. Xiong, Target of Rapamycin signaling in plant stress responses. *Plant Physiol.* 182, 1613-1623 (2020).
- M. Busche, M. R. Scarpin, R. Hnasko, J. O. Brunkard, TOR coordinates nucleotide availability with ribosome biogenesis in plants. Plant Cell 33, 1615-1632 (2021).
- Y. Liu et al., Diverse nitrogen signals activate convergent ROP2-TOR signaling in Arabidopsis. Dev. Cell 56, 1283-1295.e1285 (2021).
- H. Cho et al., ARSK1 activates TORC1 signaling to adjust growth to phosphate availability in Arabidopsis. Curr. Biol. 33, 1778-1786.e5 (2023), https://doi.org/10.1016/j.cub.2023.03.005.
- B. Menand et al., Expression and disruption of the Arabidopsis TOR (target of rapamycin) gene. Proc. Natl. Acad. Sci. U.S.A. 99, 6422-6427 (2002).
- 40. Y. Xiong, J. Sheen, Rapamycin and glucose-target of rapamycin (TOR) protein signaling in plants. J. Biol. Chem. 287, 2836-2842 (2012).
- 41. D. Deprost, H. N. Truong, C. Robaglia, C. Meyer, An Arabidopsis homolog of RAPTOR/KOG1 is essential for early embryo development. Biochem. Biophys. Res. Commun. 326, 844-850 (2005).
- 42. P. Dong et al., Expression profiling and functional analysis reveals that TOR is a key player in regulating photosynthesis and phytohormone signaling pathways in Arabidopsis. Front. Plant Sci. 6, 677 (2015).
- F. M. Hetherington, M. Kakkar, J. F. Topping, K. Lindsey, Gibberellin signaling mediates lateral root inhibition in response to K+-deprivation Plant Physiol. 185, 1198-1215 (2021).
- S. Zhao, M. L. Zhang, T. L. Ma, Y. Wang, Phosphorylation of ARF2 relieves its repression of transcription of the K+ transporter gene HAK5 in response to low potassium stress. Plant Cell 28, 3005-3019 (2016).
- X. Li et al., Differential TOR activation and cell proliferation in Arabidopsis root and shoot apexes. Proc. Natl. Acad. Sci. U.S.A. 114, 2765-2770 (2017).
- 46. D. Deprost et al., The Arabidopsis TOR kinase links plant growth, yield, stress resistance and mRNA translation. EMBO Rep. 8, 864-870 (2007).
- D. M. Gwinn et al., AMPK phosphorylation of raptor mediates a metabolic checkpoint. Mol. Cell 30, 214-226 (2008).
- 48. E. Nukarinen et al., Quantitative phosphoproteomics reveals the role of the AMPK plant ortholog SnRK1 as a metabolic master regulator under energy deprivation. Sci. Rep. 6, 31697 (2016).
- P. Wang et al., Reciprocal regulation of the TOR kinase and ABA receptor balances plant growth and stress response. Mol. Cell 69, 100-112.e106 (2018).
- N. G. Halford, S. J. Hey, Snf1-related protein kinases (SnRKs) act within an intricate network that links metabolic and stress signalling in plants. Biochem. J. 419, 247-259 (2009).
- A. K. Yadav, S. K. Jha, S. K. Sanyal, S. Luan, G. K. Pandey, Arabidopsis calcineurin B-like proteins differentially regulate phosphorylation activity of CBL-interacting protein kinase 9. Biochem. J. 475, 2621-2636 (2018)
- B. M. O'Leary, G. G. K. Oh, C. P. Lee, A. H. Millar, Metabolite regulatory interactions control plant respiratory metabolism via Target of Rapamycin (TOR) kinase activation. Plant Cell 32, 666-682 (2020).

- 53. Y. Yu et al., Sulfate-TOR signaling controls transcriptional reprogramming for shoot apex activation. New Phytol. 236, 1326-1338 (2022).
- Y. Dong et al., Sulfur availability regulates plant growth via glucose-TOR signaling. Nat. Commun. 8,
- C. Primo, A. Ferri-Blazquez, R. Loewith, L. Yenush, Reciprocal regulation of Target of Rapamycin Complex 1 and potassium accumulation. J. Biol. Chem. 292, 563-574 (2017).
- K. Deng *et al.*, Target of rapamycin regulates potassium uptake in Arabidopsis and potato. *Plant Physiol. Biochem.* **155**, 357–366 (2020).
- M. Schepetilnikov et al., GTPase ROP2 binds and promotes activation of target of rapamycin, TOR, in response to auxin. EMBO J. 36, 886-903 (2017).
- Y. Wu et al., Integration of nutrient, energy, light, and hormone signalling via TOR in plants. J. Exp. 58 Bot. 70, 2227-2238 (2019).
- R. Shin et al., The Arabidopsis transcription factor MYB77 modulates auxin signal transduction. Plant Cell 19, 2440-2453 (2007).
- Y. Cao, A. D. Glass, N. M. Crawford, Ammonium inhibition of Arabidopsis root growth can be reversed by potassium and by auxin resistance mutations aux1, axr1, and axr2. Plant Physiol. 102, 983–989

- 61. F. Vicente-Agullo et al., Potassium carrier TRH1 is required for auxin transport in Arabidopsis roots. Plant J. 40, 523-535 (2004).
- 62. C. Y. Liao et al., Brassinosteroids modulate autophagy through phosphorylation of RAPTOR1B by the GSK3-like kinase BIN2 in Arabidopsis. Autophagy 19, 1293-1310 (2023), https://doi.org/10.1080/ 15548627.2022.2124501.
- 63. L. Song et al., The RALF1-FERONIA complex interacts with and activates TOR signaling in response to low nutrients. Mol. Plant 15, 1120-1136 (2022).
- R. J. Tang, C. Wang, K. Li, S. Luan, The CBL-CIPK calcium signaling network: Unified paradigm from 20 years of discoveries. *Trends Plant Sci.* 25, 604–617 (2020).
- K. J. Livak, T. D. Schmittgen, Analysis of relative gene expression data using real-time quantitative PCR and the 2(T)(-Delta Delta C) method. *Methods* **25**, 402–408 (2001).

 R. J. Tang *et al.*, Tonoplast CBL-CIPK calcium signaling network regulates magnesium homeostasis
- in Arabidopsis. *Proc. Natl. Acad. Sci. U.S.A.* **112**, 3134–3139 (2015).
- 67. S. D. Yoo, Y. H. Cho, J. Sheen, Arabidopsis mesophyll protoplasts: A versatile cell system for transient gene expression analysis. Nat. Protoc. 2, 1565–1572 (2007).
- Q. Gao et al., RALF signaling pathway activates MLO calcium channels to maintain pollen tube integrity. Cell Res. 33, 71-79 (2023).